Available online at www.sciencedirect.com
ScienceDirect
International Journal of Solids and Structures 43 (2006) 6424–6435
INTERNATIONAL JOURNAL OF SOLIDS and STRUCTURES
www.elsevier.com/locate/ijsolstr

Multiple axial cracks in a coated hollow cylinder due to thermal shock

Xuejun Chen [a,b,*], Kun Zhang [a], Guangnan Chen [a], Gengxing Luo [a]

[a] *Laboratory of Surface Modification, Institute of Mechanics, Chinese Academy of Sciences, Beijing 100080, China*
[b] *Graduate School of the Chinese Academy of Sciences, Beijing 100080, China*

Received 1 July 2005; received in revised form 15 November 2005
Available online 6 January 2006

Abstract

The transient thermal stress problem of an inner-surface-coated hollow cylinder with multiple pre-existing surface cracks contained in the coating is considered. The transient temperature, induced thermal stress, and the crack tip stress intensity factor (SIF) are calculated for the cylinder via finite element method (FEM), which is exposed to convective cooling from the inner surface. As an example, the material pair of a chromium coating and an underlying steel substrate 30CrNi2MoVA is particularly evaluated. Numerical results are obtained for the stress intensity factors as a function of normalized quantities such as time, crack length, convection severity, material constants and crack spacing.

Keywords: Coated hollow cylinder; Thermal shock; Stress intensity factor; Multiple surface cracking

1. Introduction

It is commonly recognized that the thermal conditions, which arise during fast cooling of a solid surface, can result in tensile thermal stresses near free surface. If the condition is severe enough, sudden fracture or fatigue failure can occur. In general, two alternative failure criteria can be used to determine the severity of thermal conditions that a material can sustain without cracking (i.e., its thermal shock resistance), one based on strength (Cheng, 1951; Kingery, 1955) and the other on fracture toughness (Nied, 1983; Nied and Erdogan, 1983; Rizk and Erdogan, 1989; Hutchinson and Suo, 1992; Lu and Fleck, 1998; Zhao et al., 2000). Generally the latter treats the cases more close to the practical situations in which pre-existing cracks are assumed to exist in the solid. The single crack problems of finite-width or semi-infinite homogenous plates under convective thermal conditions were treated via the solution of singular integral equations (Nied, 1983, 1987; Rizk and Radwan, 1992). Multiple crack problems in a plate under thermal loading were considered recently in literature (Bahr et al., 1988; Rizk, 2003).

* Corresponding author. Address: Laboratory of Surface Modification, Institute of Mechanics, Chinese Academy of Sciences, No. 15 Beisihuanxi Road, Haidian District, Beijing 100080, China. Tel.: +86 10 62547527x5; fax: +86 10 62547526.
E-mail address: chenxuejuncas@sohu.com (X. Chen).

0020-7683/$ - see front matter
doi:10.1016/j.ijsolstr.2005.11.004

The single crack and multiple cracks problem of thermal shock fracture of homogenous thick-walled cylinders has been widely investigated, due to its importance to the design and manufacturing of such structural components as the pressure vessels, piping subjected to thermal transients (Oliveira and Wu, 1987; Perl and Ashkenazi, 1992; Chen and Kuo, 1994). In many modern applications, coatings are intentionally deposited on the underlying substrate to enhance some specific surface characteristics, e.g., strength, corrosion and wear resistance. The surface cracks will form inevitably in the brittle coating due to structural mismatch or thermal mismatch of coating/ substrate after the deposition process is completed. When such a system is subjected to a thermal shock, surface cracks may further propagate towards the substrate. In the absence of additional external loads and because of the self-equilibrating nature of the stress state, the cracking may not always lead to a through-thickness or catastrophic fracture. However, once the surface cracks touch on interface, detrimental effects can also be brought about. For example, during the firing process in a chromium coated gun barrel, surface cracks touching on interface will serve as convenient tunnels for corrosive gases to flow in and hence the substrate and interface will be severely attacked by erosion. Experimental results show it is a typical and common failure mechanism for such a gun barrel (Cote and Richard, 2000; Underwood et al., 2003). Therefore, it is of great significance to reduce the surface crack growth rate in an effort to prolong the total fatigue life of components. This requires the calculations of the crack driving force for the given thermal loads as a function of the crack depth and material constants. It should be pointed out that, in actual structures, the cracking analyses are usually very complicated 3-D problems. Thus for simplicity the literature concerned mainly the corresponding plane strain or plane stress problems to provide useful bounds for the actual part-through crack problem. In early 1980s, the problem of a coated hollow cylinder with a single radial or circumferential crack exposed to sudden cooling from inner surface has been treated based on numerical solution of singular integral equations (Nied and Erdogan, 1983; Tang and Erdogan, 1984, 1985). Nevertheless, it seems multiple surface cracks situation could represent practical cases more accurately and reasonably. As far as the authors know, the solution of a coated hollow cylinder with multiple surface cracks under thermal transients is not available in literature up to now. Therefore it is the main objective of the present analysis.

In this paper, the transient cracking problem of an inner-surface-coated hollow cylinder with multiple pre-existing surface cracks contained in the coating is considered. It is exposed to convective cooling from the inner surface. In solving the problem, it is assumed that both coating and substrate materials are homogeneous, isotropic and linear-elastic, the thermo-mechanical constants are independent of temperature, all thermo-elastic coupling effects and inertia effects are negligible. Previous investigations on dynamic thermo-elasticity indicated that the last assumption, which simplifies the analysis of the problem quite considerably, would not cause any significant changes in the results (Sternberg and Chakravorty, 1959; Atarashi and Minagawa, 1992). The solution of the crack problem under thermal stress may be obtained in two steps. The first step would be the calculation of time-dependent temperature field and induced thermal stress. Then the results in the first step would serve as input data to SIF evaluation. In fact, there exists a closed form solution for the temperature and thermal stress in the above cylinder, in the form of an infinite series of Bessel functions and Neumann functions (Tang and Erdogan, 1984, 1985). For convenience, all the calculations in this paper are completed via the finite element method (FEM). Numerical results for stress intensity factors are obtained as a function of normalized quantities such as time, convection severity, crack length, material constants as well as crack spacing.

2. Problem formulation

The problem of a coated hollow cylinder is considered, with cylindrical coordinates (r, ϕ, z) embedded at its center, as shown in Fig. 1. This plane strain problem with multiple pre-existing surface cracks represents a reasonable idealization for the stresses and displacements in the central portion of a cracked coated cylinder. It also gives the upper bound solution for practical 3-D geometry. The cylinder of inner radius a, outer radius b and coating thickness h, at an initial temperature T_0, is assumed to be perfectly insulated along the outside surface $r = b$. The inner surface at $r = a - h$ contains n radial cracks of depth l (only four cracks are plotted in Fig. 1.).

At time $t = 0$, the inner surface is subjected to convective cooling with the heat transfer coefficient given by H and the ambient temperature maintained at T_a. By nature of axis-symmetry, temperature and thermal stress

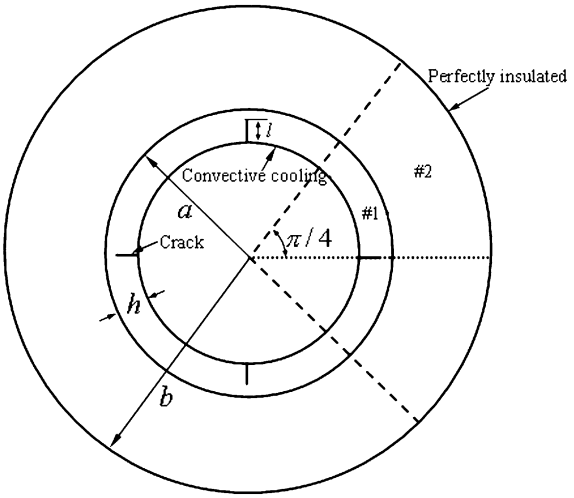

Fig. 1. The multi-cracked and coated cylinder subjected to convective cooling from inner surface.

components are largely simplified to depend only on r and t, i.e., 1-D thermal diffusion problem. The formulation of the mixed boundary value problem needed for the solution of the cracking problem in Fig. 1 can utilizes the transient thermal stress distribution from the un-cracked hollow cylinder due to the fact that the existence of multiple radial cracks would not cause any disturbance in temperature field throughout the coated hollow cylinder. Further, partial derivative $\partial/\partial\phi$ vanishes and there exist only three non-zero stress components σ_{rr}, $\sigma_{\phi\phi}$ and σ_{zz}.

When the coated hollow cylinder is exposed to convective cooling from inner surface $r = a - h$, tensile circumferential stress would develop near the inner surface due to subsequent positive temperature gradient in the radial direction and stress intensity would then build near the crack tips. Apparently only circumferential stress component $\sigma_{\phi\phi}$ contributes to the mode I stress intensity factors for surface cracks; hence emphasis is solely placed on component $\sigma_{\phi\phi}$ in thermal stresses calculation. The transient temperature distribution may be determined from the solution of the diffusion equations

$$\nabla^2\theta_i(r,t) = \frac{1}{D_i}\frac{\partial\theta_i(r,t)}{\partial t} \quad (i = 1,2) \tag{1}$$

where temperature changes θ_i are defined by

$$\theta_i(r,t) = T_i(r,t) - T_0 \quad (i = 1,2) \tag{2a}$$

$$\theta_0 = T_a - T_0 \tag{2b}$$

The subscripts 1, 2 represent coating and substrate, respectively. The thermal diffusivity D_i is given by $D_i = k_i/\rho_i c_i$, where k_i is the material thermal conductivity, ρ_i the density and c_i the specific heat. T_0 is the initial temperature throughout the coated hollow cylinder. In the case of convective cooling, $\theta_0 < 0$.

The initial conditions are given by

$$\theta_1(r,0) = 0 \quad (a - h < r < a) \quad \theta_2(r,0) = 0 \quad (a < r < b) \tag{3}$$

The continuity and boundary conditions are usually written as

$$\theta_1(a,t) = \theta_2(a,t), \quad k_1\frac{\partial}{\partial r}\theta_1(a,t) = k_2\frac{\partial}{\partial r}\theta_2(a,t) \quad (t > 0) \tag{4a}$$

$$\frac{\partial}{\partial r}\theta_1(a-h,t) = \frac{H}{k_1}[\theta_1(a-h,t) - \theta_0], \quad \frac{\partial}{\partial r}\theta_2(b,t) = 0 \quad (t > 0) \tag{4b}$$

It is emphasized that Eq. (4a) indicates the continuity of temperature and heat flux at the coating/substrate interface, neglecting contact thermal resistance.

Bearing in mind the usual equilibrium, constitutive and geometrical equations, which can be easily found in any thermo-elasticity textbook, we write the following boundary and continuity conditions for thermal stress calculations

$$\sigma_{rr1}(a-h,t)=0;\sigma_{rr2}(b,t)=0 \quad (t>0) \tag{5a}$$

$$u_{r1}(a,t)=u_{r2}(a,t);\sigma_{rr1}(a,t)=\sigma_{rr2}(a,t) \quad (t>0) \tag{5b}$$

where u_r and σ_{rr} denote radial displacement and radial stress component, respectively. It is feasible to calculate the mode I stress intensity factor as usual by specifying cracks' faces as free boundaries or by principle of superposition in which the crack surface tractions equal and opposite to the thermal stresses in the un-cracked cylinder are the only external loads (Schulze and Erdogan, 1998; Rizk, 2003). For convenience of the use of FE method here, the latter is chosen.

3. Solution procedures

3.1. Dimensional analysis

Prior to the specific solution to the above problem is known, dimensional analysis can be carried out to reveal the scaling relationships of this problem. From Eqs. (1–4), the temperature changes $\theta_i (i=1,2)$ must be functions of all the independent governing parameters, i.e., temporal and spatial quantities t and r; characteristic geometrical parameters a, b and h; thermo-physical constants D_1, D_2, k_1, k_2, H and initial temperature θ_0

$$\theta_i(r,t)=f(r,t;a,h,b;D_1,D_2,k_1,k_2,H;\theta_0) \tag{6}$$

Among the twelve governing parameters, four of them, namely h, D_1, k_1 and θ_0, has independent dimensions. The dimensions of θ_i, r, t, a, b, D_2, k_2 and H are given by

$$\begin{aligned}
&[\theta_i]=[\theta_0]\\
&[r]=[h]\\
&[t]=[D_1]^{-1}[h]^2\\
&[a]=[h]\\
&[b]=[h]\\
&[D_2]=[D_1]\\
&[k_2]=[k_1]\\
&[H]=[k_1][h]^{-1}
\end{aligned} \tag{7}$$

On applying Π-theorem in dimensional analysis (Barenblatt, 1996), we obtain

$$\frac{\theta_i}{\theta_0}=\Pi_\theta\left(\frac{r}{h},\frac{D_1 t}{h^2};\frac{a}{h},\frac{b}{h};\frac{D_2}{D_1},\frac{k_2}{k_1},\frac{Hh}{k_1}\right) \tag{8}$$

The following dimensionless quantities are then naturally defined as

$$\begin{aligned}
&\bar{r}=\frac{r}{h} \quad \bar{a}=\frac{a}{h} \quad \bar{b}=\frac{b}{h} \quad \overline{D}=\frac{D_2}{D_1}\\
&\bar{k}=\frac{k_2}{k_1} \quad Bi=\frac{Hh}{k_1} \quad Fo=\frac{D_1 t}{h^2}
\end{aligned} \tag{9}$$

Based on the above dimensional analysis, the dimensionless quantity θ_i/θ_0 on the left side of Eq. (8) is determined only by seven bracketed dimensionless quantities on the right side, in which Bi and Fo are similar to Biot number and Fourier number, respectively. The most severe thermal shock case corresponds to a sudden cooling, i.e., $Bi \to \infty$.

Similarly, stress components depend on the following quantities

$$\sigma(r,t)=g(r,t,\theta_0;a,h,b;D_1,D_2,k_1,k_2,H;E_1,E_2,\nu_1,\nu_2,\alpha_1,\alpha_2) \tag{10}$$

On applying Π-theorem again, we obtain

$$\frac{-(1-\nu_1)\sigma}{E_1\alpha_1\theta_0} = \Pi_\sigma\left(\frac{r}{h},\frac{D_1 t}{h^2};\frac{a}{h},\frac{b}{h};\frac{D_2}{D_1},\frac{k_2}{k_1},\frac{Hh}{k_1};\frac{E_2}{E_1},\frac{\nu_2}{\nu_1},\frac{\alpha_2}{\alpha_1}\right) \tag{11}$$

As can be shown by Eq. (11), three additional dimensionless quantities, $\overline{E} = E_2/E_1$, $\bar{\nu} = \nu_2/\nu_1$ and $\bar{\alpha} = \alpha_2/\alpha_1$ should appear automatically in thermal stress analysis, which measure substrate and coating's relative value of Young's modulus, Poisson's ratio and thermal expansion coefficient, respectively.

In terms of time-dependent thermal stress, mode I stress intensity factor for multiple surface cracks is also time-dependent. When it comes to the normalized expression, dimensionless crack depth $\bar{l} = l/h$ and crack spacing $\bar{s} = s/h$ should be added into corresponding function, i.e.,

$$K(t) = \gamma(t,\theta_0;a,h,b,l;D_1,D_2,k_1,k_2,H;E_1,E_2,\nu_1,\nu_2,\alpha_1,\alpha_2;s) \tag{12}$$

$$\frac{-(1-\nu_1)K}{E_1\alpha_1\theta_0\sqrt{h}} = \Pi_K\left(\frac{D_1 t}{h^2};\frac{a}{h},\frac{b}{h},\frac{l}{h};\frac{D_2}{D_1},\frac{k_2}{k_1},\frac{Hh}{k_1};\frac{E_2}{E_1},\frac{\nu_2}{\nu_1},\frac{\alpha_2}{\alpha_1};\frac{s}{h}\right) \tag{13}$$

where $s \equiv 2\pi(a-h)/n$ and n is the assumed crack numbers. With the help of the above dimensional analysis, sensitivity analysis for temperature, thermal stress and mode I stress intensity factor can be conveniently performed, which will be detailed in Section 4.

3.2. Finite element model

Since the above non-homogeneous mixed boundary problem has currently no analytical solution, we resort to finite element method. For convenience, the number of surface cracks is considered in the FE model as it correlates inversely with crack spacing. In the case of an array of n surface cracks evenly spaced and of equal depth l, only a sector of the coated hollow cylinder, with a central angle of π/n, has to be considered due to the symmetry of the problem. As the number of cracks in the array increases, the geometry of the sector becomes slender and slender. In order to obtain accurate results, careful element meshing is necessary to assure a reasonable aspect ratio of the elements, and particularly element refinements should be done in the vicinity of the crack tip and the interface of coating and substrate. The detailed mesh breakdowns are illustrated in Fig. 2. The associated boundary conditions in Fig. 2 should be understood as follows: (i) For the temperature calculation, perfect insulation ($dT/dn = 0$) is imposed on circumferential direction; (ii) For the thermal stress calculation, the vanishing circumferential displacement is added; (iii) For the SIF calculation, the crack faces are free.

Each of the sectors is divided into 1168–8724 elements in terms of different crack numbers. Eight-node isoparametric quadrilateral and six-node quadratic interface elements are used here for both displacement and temperature calculations. In linear elastic problems, it has been shown that the displacements near the crack

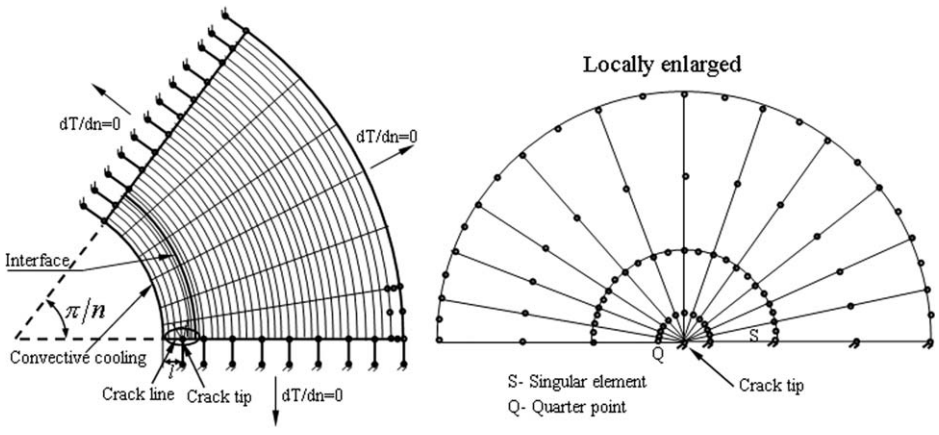

Fig. 2. The schematic of finite element meshes and boundary conditions in the analysis.

Table 1
The comparisons of some results for homogeneous, hollow cylinder

F	0.0005	0.002	0.01	0.03	0.07	0.1
$\overline{K}$	0.151	0.239	0.281	0.261	0.252	0.245
$\overline{K}^1$	0.167	0.250	0.298	0.273	0.261	0.251
$\overline{K}^2$	0.145	0.234	0.279	0.256	0.248	0.239

It is subjected to sudden cooling from the inner surface while outer surface is kept at the initial temperature. $a/b = 0.5$, $h = 0$, $n = 2$, $W = b - a$, $l/W = 0.05$, $F = Dt/a^2$, $\overline{K} = K/K_0$, $K_0 = E\alpha\Delta T\sqrt{W}/(1-\nu)$. $\overline{K}$, $\overline{K}^1$ and $\overline{K}^2$ is the result of current paper, Oliveira and Wu, and Perl and Ashkenazi, respectively.

tip vary as $\sqrt{r}$, where r is the distance from the crack tip. The stresses and strains are singular at the crack tip, varying as $1/\sqrt{r}$. To pick up the singularity in the strain, the crack faces should be coincident, and the elements around the crack tip should be quadratic, with mid-side nodes placed at the quarter points, known as singular elements. The quarter points and the singular elements surrounding the crack tip are labeled in Fig. 2 as Q and S, respectively. The first row of elements around the crack tip should be singular, the radius of which is chosen to be one tenth of quadrilateral element length, and the number of elements in the local circumferential direction is taken to be twelve. With the temperature distribution in the cylinder known, it is easy to determine the transient thermal stress by the classical finite element formulation. The stress intensity factor is extracted from the FE solution via the circumferential displacement u_ϕ at the quarter point of the singular element on the free face of the crack. This relation can be expressed as follows (Lynn and Ingraffea, 1978)

$$K_I = \frac{E_i u_\phi}{(1+\nu_i)(1+\kappa_i)}\left(\frac{2\pi}{r_q}\right)^{1/2} \tag{14}$$

where r_q is the distance from quarter point to the crack tip, $i = 1$ when crack tip is within the coating while $i = 2$ within the substrate and $\kappa_i = 3 - 4\nu_i$ in the case of plane strain problem. By letting the coating and substrate have the same material constants and $Bi \to \infty$, a series of runs were performed to duplicate various results obtained by Oliveira and Wu (1987), which was obtained via method of weight function and by Perl and Ashkenazi (1992), which was obtained also by FE method. Most of the results were found to be in excellent agreement with those in references (see Table 1). Hence the present FE model is reasonably validated.

4. Numerical results and discussions

As an example for the thermal shock problem described in the previous sections, we consider a material pair, which corresponds to a chromium coating deposited onto a much thicker structural steel substrate 30CrNi2MoVA. Since the problem is formulated in terms of dimensionless quantities, it is sufficient to consider only the ratios shown in the Table 2. Unless otherwise stated, we have taken data from Table 2 in our calculations whenever the required input quantities are not shown. All the quantities of interest are normalized in the same forms as those in Section 3.1.

The normalized transient temperature distributions in the un-cracked, coated hollow cylinder are shown in Figs. 3 and 4 and a dash-dot line is embedded in both figures to indicate the "physical" low and high temperature region along ordinate. At various time instants, the variation of normalized temperature versus normalized radial coordinate is plotted in Fig. 3. It is shown that, the normalized temperature intractably decreases with normalized time and such a trend constantly penetrates into the coated cylinder. The normalized temperature gradient within the coating is also a decreasing function of normalized time until steady state is reached. At the coating/substrate interface, the slope of curve discontinues, indicating the different thermal resistances of coating and substrate. In order to investigate the effect of convection severity on normalized temperature

Table 2
The dimensionless quantities used in the example

a/h	b/h	D_2/D_1	k_2/k_1	E_2/E_1	ν_2/ν_1	α_2/α_1	Fo	Bi
100	200	0.293	0.389	0.724	1.476	1.923	3	0.225

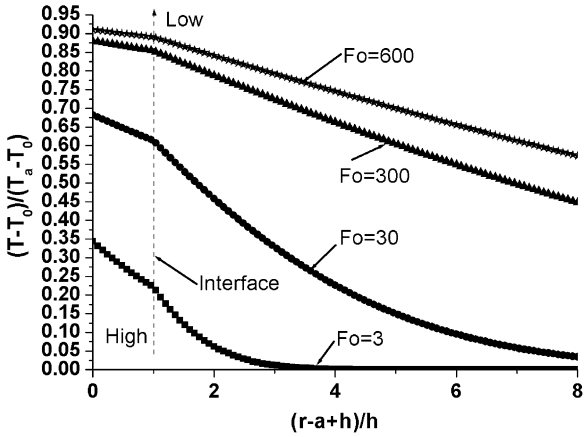

Fig. 3. The normalized transient temperature versus normalized radial coordinate for various time instants, $Bi = 0.225$. Other inputs are listed in Table 2.

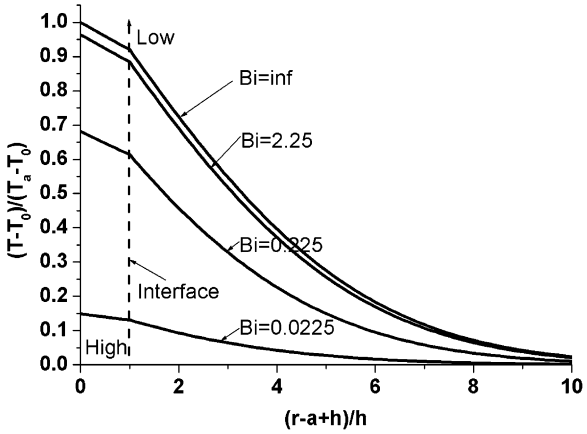

Fig. 4. The normalized transient temperature versus normalized radial coordinate for various Biot numbers, $Fo = 30$. "inf" stands for "∞". Other inputs are listed in Table 2.

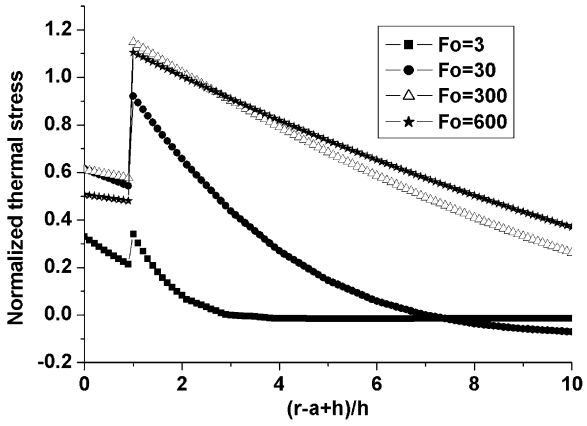

Fig. 5. The variation of normalized circumferential stress $\sigma_{\phi\phi}$ versus normalized radial coordinate for different time instants, $Bi = 0.225$. Other inputs are listed in Table 2.

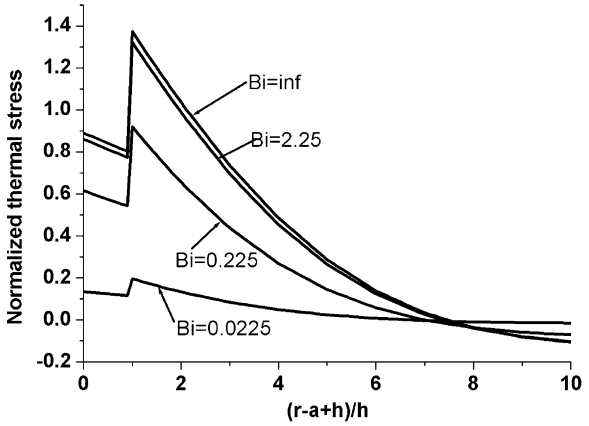

Fig. 6. The variation of normalized circumferential stress $\sigma_{\phi\phi}$ versus normalized radial coordinate for different Biot numbers, $Fo = 30$. "inf" stands for "∞". Other inputs are listed in Table 2.

distribution, different Biot numbers were chosen in Fig. 4 to find that, the increase of Biot number could significantly reduce the normalized temperature throughout the coated hollow cylinder, especially notable in the vicinity of inner surface.

Some results concerning normalized thermal stress distribution are shown in Figs. 5 and 6. In Fig. 5 the variation of normalized transient circumferential stress component $\sigma_{\phi\phi}$ versus normalized radial coordinate is plotted for different values of normalized time instants. It can be seen the coating invariably experiences tensile stress component $\sigma_{\phi\phi}$. In terms of the discrepancies of thermo-physical properties of coating and substrate, circumferential stress discontinues at the interface as expected. Due to the self-equilibrating nature of thermal stress, there exist compressive stress region somewhere more far away from the inner surface. It should be emphasized that, compared to twice sign changes of thermal stresses for the finite-width plates under similar thermal conditions (Nied and Erdogan, 1983), there is only once sign change here for hollow cylinder geometries. As the time elapses, the normalized tensile thermal stress component $\sigma_{\phi\phi}$ in the coating first increases up to a peak value then decreases until the problem reaches the steady state. This change trend is in favorable agreement with corresponding time-dependent normalized temperature distribution in Fig. 3. It can also be shown that normalized circumferential thermal stress distribution in the coating is not always uniform and the maximum and minimum magnitude at small time instant can differ by about 30%. Fig. 6 demonstrates the effect of convection severity on the normalized circumferential thermal stress. From it we can see, the induced normalized tensile thermal stress near the inner surface increases with the increase of Biot number while larger normalized compressive stress is generated in the core of the substrate.

Some results of crack driving force, represented by normalized mode I stress intensity factor, are plotted in Figs. 7–11. In Fig. 7 the variation of normalized stress intensity factor versus normalized time for various crack depths is plotted. From it we can see, for a given crack depth the normalized stress intensity factor first increases sharply with time up to the peak value $K_{\max}$, followed by docile decrease. From point view of linear elastic fracture mechanics (LEFM), the crack extension would always stop when the fracture toughness of coating is high enough to exceed $K_{\max}$.Therefore the most dangerous moment the cylinder experience is not at steady state of thermal loading, but at some intermediate instant. This variation trend can be interpreted by corresponding temperature gradient and thermal stress variation described previously. Fig. 7 also shows that, for the surface cracks within the coating, as the normalized crack depth increases, the normalized stress intensity factor also increases monotonously at any instant. Fig. 8 illustrates the effect of modulus ratio on the normalized stress intensity factor, indicating the increase of modulus ratio can cause the decrease of crack driving force and the possibility of crack extension. This effect was also previously validated by Hutchinson and Suo (1992). However, it would not seem so notable upon further increase of modulus ratio. It is shown in Fig. 9 that, the normalized stress intensity factor is almost a linearly decreasing function of normalized ratio of coefficients of thermal expansion $\bar{\alpha} = \alpha_2/\alpha_1$. This indicates for a given substrate the reduction of coefficient

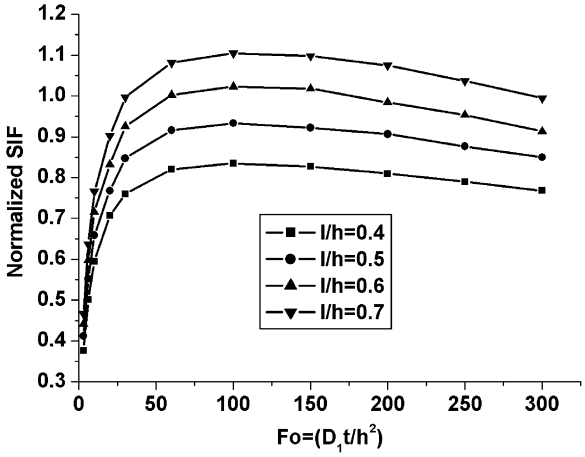

Fig. 7. The variation of normalized stress intensity factor versus normalized time for different crack depths, $n = 4$, $Bi = 0.225$. Other inputs are listed in Table 2.

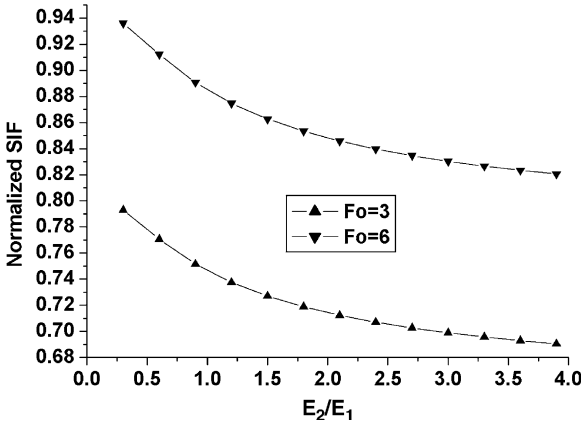

Fig. 8. The effect of normalized modulus ratio on normalized stress intensity factor at different instants, $n = 4$, $l/h = 0.5$, $Bi = 0.675$. Other inputs are listed in Table 2.

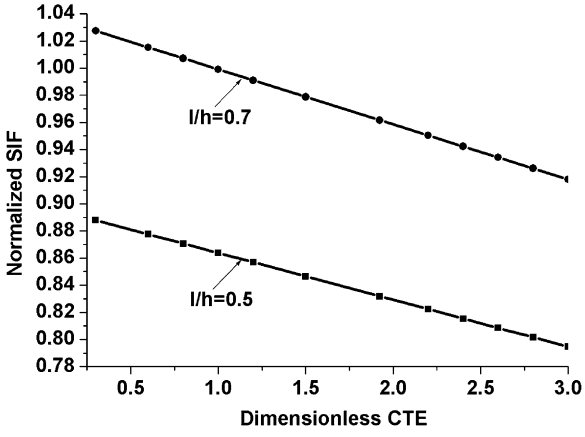

Fig. 9. The effect of normalized CTE on normalized stress intensity factor, $n = 30$, $Bi = 0.225$, $Fo = 30$. Other inputs are listed in Table 2.

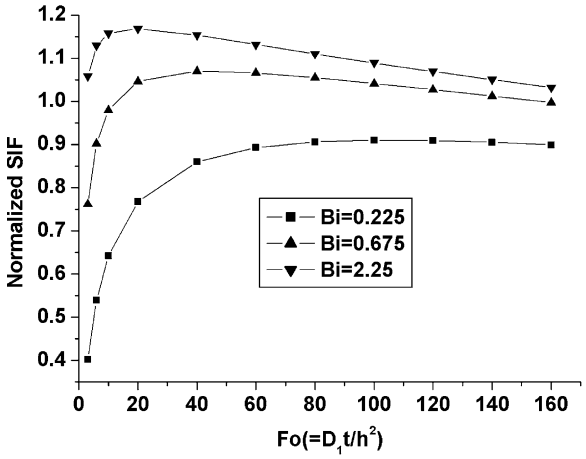

Fig. 10. The variation of normalized stress intensity factor versus normalized time for different Biot numbers, $l/h = 0.5$, $n = 4$. Other inputs are listed in Table 2.

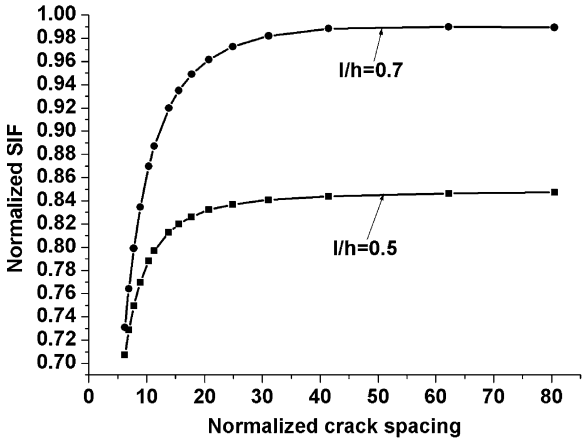

Fig. 11. The variation of normalized stress intensity factor versus normalized crack spacing, $Bi = 0.225$, $Fo = 30$. Other inputs are listed in Table 2.

of thermal expansion (CTE) of coating may lead to reduction for crack driving force. Also, the slope of the line remains almost constant for different crack lengths. Fig. 10 demonstrates the influence of convection severity measured by Biot number on the normalized stress intensity factor. As more severe thermal shock is applied, the magnitude of normalized stress intensity factor becomes larger and the moment at which the peak stress intensity factor occurs comes earlier. It seems even more significant for small values of time. Finally, the variation of the normalized stress intensity factor versus normalized crack spacing $\bar{s} = s/h$ for various crack lengths is plotted in Fig. 11. It is shown that for a given normalized crack depth, the magnitude of stress intensity factor first decreases slightly with the decrease of normalized crack spacing, followed by sharp decrease with further decrease of normalized crack spacing. This change trend can be understood as follows: when crack spacing is very large with small crack numbers, the interaction between multiple cracks is little; when crack spacing becomes smaller and smaller, the redistribution of thermal stress induced by the introduction of multiple cracks generates "shedding effect", causing the decrease of stress intensity in the vicinity of the crack tip. Thus, if only a single crack is assumed in the associated analysis, the result for the crack driving force will obviously overestimate the practical situations. This interesting and important phenomenon is also termed as "load relief effect" in previous literature (Rooke et al., 1981; Parker, 1999).

5. Conclusions

In this paper, the transient cracking problem of an inner-surface-coated hollow cylinder with multiple pre-existing surface cracks contained in the coating is considered. It is exposed to convective cooling from the inner surface. As an example, the material pair of a chromium coating and an underlying steel substrate 30CrNi2MoVA is particularly analyzed to assess the effect of some infectious factors on the stress intensity factor. Results indicate the crack spacing appears to be an important parameter in the variation of the stress intensity factor. By decreasing the crack spacing, the stress intensity factor becomes smaller in magnitude. For small values of time, convection severity measured by Biot number is quite significant. Not only can it increase the stress intensity factor, but the peak stress intensity factor will occur earlier. Other factors conducive to the reduction of stress intensity factor for a given substrate include the decrease of crack depth, coating's modulus and coating's coefficient of thermal expansion.

Acknowledgments

The financial support provided by the National Natural Science Foundation of China (Grant No. 50471087, 50531060) is greatly acknowledged. We also want to express our deep gratitude to reviewers for their constructive suggestions.

References

Atarashi, T., Minagawa, S., 1992. Transient coupled-thermoelastic problem of heat conduction in a multilayered composite plate. International Journal of Engineering Sciences 30 (10), 1543–1550.

Bahr, H.A., Weis, H.J., Maschke, H.G., Meissner, F., 1988. Multiple crack propagation in a strip caused by thermal shock. Theoretical and Applied Fracture Mechanics 10, 219–226.

Barenblatt, G.I., 1996. Scaling, Self-similarity, and Intermediate Asymptotics. Cambridge University Press, Cambridge.

Chen, C., Kuo, B., 1994. Transient thermal contact problem for an infinite edge crack in a layered cylinder. Engineering Fracture Mechanics 49 (3), 381–392.

Cheng, C.M., 1951. Resistance to thermal shock. Journal of the American Rocket Society 21, 147–153.

Cote, P.J., Richard, C., 2000. Gas-metal reaction products in the erosion of chromium-plated gun bores. Wear 241, 17–25.

Hutchinson, J.W., Suo, Z., 1992. Mixed-mode cracking in layered materials. Advances in Applied Mechanics 29, 63–187.

Kingery, W.D., 1955. Factors affecting thermal stress resistance of ceramic materials. Journal of the American Ceramic Society 38, 3–10.

Lu, T.J., Fleck, N.A., 1998. The thermal shock resistance of solids. Acta Materialia 46 (13), 4755–4768.

Lynn, P.P., Ingraffea, A.R., 1978. Transition elements to be used with quadratic point crack tip elements. International Journal for Numerical Methods in Engineering 12, 1031–1038.

Nied, H.F., 1983. Thermal shock fracture in an edge-cracked plate. Journal of Thermal Stresses 6, 217–229.

Nied, H.F., 1987. Thermal shock in an edge-cracked plate subjected to uniform surface heating. Engineering Fracture Mechanics 26 (2), 239–246.

Nied, H.F., Erdogan, F., 1983. Transient thermal stress problem for a circumferentially cracked hollow cylinder. Journal of Thermal Stresses 6, 1–14.

Oliveira, R., Wu, X.R., 1987. Stress intensity factors for axial cracks in hollow cylinders subjected to thermal shock. Engineering Fracture Mechanics 27 (2), 185–197.

Parker, A.P., 1999. Stability of arrays of multiple edge cracks. Engineering Fracture Mechanics 62, 577–591.

Perl, M., Ashkenazi, A., 1992. A more realistic thermal shock analysis of a radially multicracked thick-walled cylinder. Engineering Fracture Mechanics 42 (5), 747–756.

Rizk, A.A., 2003. Transient stress intensity factors for periodic array of cracks in a half-plane due to convective cooling. Journal of Thermal Stresses 26, 443–456.

Rizk, A.A., Erdogan, F., 1989. Cracking of coated materials under transient thermal stresses. Journal of Thermal Stresses 12, 125–168.

Rizk, A.A., Radwan, S.F., 1992. Transient thermal stress problem for a cracked semi-infinite medium. Journal of Thermal Stresses 15, 451–468.

Rooke, D.P., Baratta, F.I., Cartwright, D.J., 1981. Simple methods of determining stress intensity factors. Engineering Fracture Mechanics 14, 397–426.

Schulze, G.W., Erdogan, F., 1998. Periodic cracking of elastic coatings. International Journal of Solids and Structures 35, 3615–3634.

Sternberg, E., Chakravorty, J.G., 1959. On the inertia effects in a transient thermoelastic problem. ASME Journal of Applied Mechanics 26, 503–509.

Tang, R., Erdogan, F., 1984. Stress intensity factors in a reinforced thick-walled cylinder. International Journal of Engineering Sciences 22, 867–879.

Tang, R., Erdogan, F., 1985. Transient thermal stresses in a reinforced hollow disk or cylinder containing a radial crack. Journal of Engineering for Gas Turbines and Power 107, 212–219.

Underwood, J.H., Park, A.P., Vigllante, G.N., Cote, P.J., 2003. Thermal damage, cracking and rapid erosion of cannon bore coatings. Journal of Pressure Vessel Technology 125 (3), 299–304.

Zhao, L.G., Lu, T.J., Fleck, N.A., 2000. Crack channeling and spalling in a plate due to thermal shock loading. Journal of the Mechanics and Physics of Solids 48, 867–897.